

## Organic carbon flux and organic carbon to calcite flux ratio recorded in deep-sea carbonates: Demonstration and a new proxy

Figen A. Mekik

Department of Geology, Grand Valley State University, Allendale, Michigan, USA

Paul W. Loubere

Department of Geology and Environmental Geosciences, Northern Illinois University, De Kalb, Illinois, USA

David E. Archer

Department of Geophysical Sciences, University of Chicago, Chicago, Illinois, USA

Received 18 September 2001; revised 19 April 2002; accepted 19 April 2002; published XX Month 2002.

[1] Theoretical considerations indicate that degree of bottom water calcite saturation, organic carbon flux, and the ratio of that flux to the calcite flux all are reflected in the carbonate preservation record of deep-sea sediments. Separating the influence of these various factors on the record depends first on estimating the percent of the calcite flux which is dissolved at the seabed. We have developed a new proxy for percent dissolved calcite by calibrating a foraminiferal fragmentation index to biogeochemical model-derived data. Application of our proxy, combined with geochemical modeling, to the surface sediments of the Eastern Equatorial Pacific [EEP], demonstrates the need for all three of the variables listed above to account for the observations. Further, we used reverse modeling to map the ratio of the biotic fluxes across the EEP. We observe a coherent regional pattern with highest ratio values, as expected, associated with areas of upwelling, particularly along South America. Our proxy appears to be unaffected by carbonate sediment properties such as percent calcite in samples or the amount of coarse fraction ( $>63 \mu\text{m}$ ) in the calcareous portion of the sediments; therefore it reflects primarily the geochemical environment rather than characteristics of seabed deposits. *INDEX TERMS*: 4231 Oceanography: General: Equatorial oceanography; 4805 Oceanography: Biological and Chemical: Biogeochemical cycles (1615); 4806 Oceanography: Biological and Chemical: Carbon cycling; 4842 Oceanography: Biological and Chemical: Modeling; *KEYWORDS*: calcite dissolution, marine carbon fluxes, marine calcite rain, foraminiferal preservation, biogeochemical modeling, eastern equatorial Pacific

### 1. Introduction

[2] The carbonate record of the deep ocean has attracted attention for decades as it reflects properties of deep ocean water masses, surface ocean bioproductivity, and important aspects of the global carbon cycle. A feature of the carbonate record that was recognized nearly 50 years ago is the cyclic preservation of carbonates in deep-sea sediments. *Arrhenius* [1952] attributed these variations in preservation to changing flux of particles to the seabed. Fluctuations in carbonate chemistry of deep waters were considered as an alternative driving mechanism for these cycles [*Broecker*, 1971; *Berger*, 1973](see also review by *Berger* [1992]). Later, changes in deep-sea chemistry coupled with biotic carbonate flux were integrated into models of ocean response to climate change [e.g., *Broecker*, 1982; *Berger and Keir*, 1984]. Most recently, carbonate cycles in deep-sea sediments have been examined in terms

of processes that could change the carbon dioxide concentration of the atmosphere, since this is an important climate variable on the glacial/interglacial timescale for which there is presently no good explanation [e.g., *Archer and Maier-Reimer*, 1994; *Archer et al.*, 2000].

[3] There are three main variables controlling the deep-sea carbonate preservation system: bottom water carbonate chemistry, carbonate flux to the seabed, and organic carbon flux from the oceanic euphotic zone. *Archer et al.* [1989] and *Archer* [1991a, 1991b], following on work by *Emerson and Bender* [1981] and followed by *Hales and Emerson* [1996, 1997a, 1997b], showed that flux of organic matter to the seabed is as important to calcite preservation as is the bottom water carbonate chemistry. Calcite dissolution then becomes a function of the ratio of organic carbon flux to calcite flux. Further, this ratio has a potentially important effect on atmospheric carbon dioxide concentration [*Archer and Maier-Reimer*, 1994].

[4] Examining these interacting factors in the past is a problem, but it could be accomplished with accurate estimates of paleofluxes. The paleoflux of calcite can be

calculated if an estimate of the fraction of the calcite flux that was dissolved at the seafloor can be made, and calcite accumulation rates at the seabed are measured. Also, estimates of paleo-organic carbon flux, combined with estimates of bottom water calcite saturation, would make possible model calculations of dissolution fluxes. This combined with estimates of percent calcite dissolved could then be used to estimate paleo-ratios of organic carbon to calcite fluxes. Naturally, measurement of paleo-calcite and organic carbon fluxes at the seabed would allow direct calculation of organic carbon flux to calcite flux ratios. At the very least, it should be possible to examine directions of paleo-ratio change in the past. Alternatively, estimation of calcite and organic carbon fluxes, along with measurement of percent calcite dissolved, could be used to examine, through modeling, changes in bottom water calcite saturation through time. Attempts to quantify the fluxes and their ratio are important both for understanding surface ocean plankton community response to climate change, and for determining changes in the marine carbonate system that are important to the global carbon cycle.

[5] We present a new method for reconstructing the fraction of calcite flux to the seafloor which is dissolved and we test this method with surface sediment samples (representing the modern ocean) from the eastern equatorial Pacific to demonstrate that bottom water calcite saturation, organic carbon flux and the organic carbon to calcite flux ratio are all recorded in the sediments. We then show that the sediment record can be used to reconstruct past calcite fluxes, and changes in the flux ratio through time.

## 2. Quantifying Dissolution

[6] We have developed a simple, time-efficient sedimentary index for estimating the fraction of calcite dissolved in a given sample and calibrated our index with values derived from biogeochemical modeling. Many sedimentary indices for calcite dissolution already exist as quantifying calcite dissolution has been a long-standing oceanographic problem. We use the fragmentation of *Globorotalia menardii*, a planktic foraminifer, as our sedimentary index. Our proxy is unique, however, in that we can anchor our foraminiferal fragmentation index with model-derived percent calcite dissolved values. Further, our proxy would allow for estimating paleo-calcite flux for down-core samples if accumulation rates for these samples can be quantified by independent means. The paleo-calcite flux would be paleo-calcite flux = accumulation rate/(1 - fraction dissolved).

### 2.1. Previous Sedimentary Indices of Calcite Dissolution

[7] The observation that carbonate dissolution increases with water depth goes as far back as the Challenger Expedition where John Murray first noticed a bathymetric control on the preservation of calcareous fossils (Murray and Renard [1891], cited by Berger [1975]). Arrhenius [1952] introduced foraminiferal fragmentation as a quantitative index of dissolution. Various quantitative dissolution indices have been developed after Bramlette's [1961] recognition of the Carbonate Compensation Depth [CCD],

Peterson's [1966] buoy experiments which established the presence of a hydrographic zone of increasing carbonate dissolution with depth above the saturation horizon (hydrographic lysocline), and the recognition that dissolution of larger foraminifera mostly occurs at the sediment water interface and not during settling through the water column [Adelseck and Berger, 1975]. The first two of these indices are the compositional change in planktic foraminiferal faunas with dissolution [Berger, 1967; Ruddiman and Heezen, 1967] and the degree of fragmentation of foraminiferal tests [Berger, 1970]. Since warm water taxa tend to have more delicate tests, assemblages affected by dissolution become richer in cold-water forms [Berger, 1968]. This bias in the sedimentary record led many researchers to develop methods of quantifying dissolution and correcting transfer functions for estimating SST [e.g., Miao et al., 1994; Le and Thunell, 1996].

[8] From the recognition of dissolution-modified planktic foraminifera assemblages grew the method of ranking planktic taxa by their susceptibility to dissolution [Berger, 1970; Thunell and Honjo, 1981], and of using the ratio of more susceptible to more resistant forms [Berger, 1970; Thompson and Saito, 1974] to document the effects of dissolution. Berger's Dissolution Index (BDI [Berger, 1968, 1970; Le and Shackleton, 1992]) uses this ranking to define an index of dissolution.

[9] Compositional criteria, such as the BDI, for quantifying dissolution are influenced by ecological factors [Bé et al., 1975], however, and Thunell [1976] suggested that the benthic/planktic foraminiferal ratio and the degree of fragmentation of planktic foraminifera are the best quantifiers of dissolution. Oba [1969] found that the ratio of fragmented to whole *Globorotalia menardii* shells correlates well with benthic to planktic ratios. Ku and Oba [1978] subsequently calibrated carbonate weight loss to attrition of *G. menardii* tests in laboratory experiments. This is the initial basis for our use of this species. In their experiments they concurrently dissolved a sample of perfect, undamaged, *G. menardii* shells and a sample of ooze sediment with a series of acid treatments and developed a near-linear scale for percent calcite dissolved within  $\pm 2.5$ –5%. The advantage they point out in using *G. menardii* tests only is the elimination of problems associated with initial abundance or composition produced by studying varied foraminiferal assemblages. Finally, Metzler et al. [1982] demonstrated that fragmentation is a more reliable index than carbonate weight loss in the coarse fraction ( $>177 \mu\text{m}$ ).

[10] Although many studies use percent carbonate as a preservation index, this parameter is not solely controlled by the dissolution of carbonate, but also by surface ocean productivity, calcite flux and dilution by noncarbonate materials [Ruddiman, 1971; Berger, 1992]. Thompson and Saito [1974] could not find any correlation between carbonate content of samples and observed dissolution cycles in the eastern equatorial Pacific.

[11] Peterson and Prell [1985a, 1985b] developed a composite dissolution index [CDI] by applying R-mode factor analysis to six dissolution indices: weight percent of carbonate, coarse fraction percent greater than  $63 \mu\text{m}$ , percent of whole planktic foram tests, benthic/planktic

ratios, percent of whole *G. menardii* tests, and percent of radiolarians relative to foraminifers. Using the CDI on samples from the eastern equatorial Indian Ocean, *Peterson and Prell* [1985a] concluded that supralysocline dissolution is significant and most probably driven by organic carbon degradation at the seabed, whereas dissolution below the depth of calcite saturation in the water column is controlled more by deep water chemistry. It is important to note that supralysocline dissolution has a greater effect on the relative preservation of foraminifera in the coarse fraction than on total carbonate loss [*Peterson and Prell*, 1985a]. Thus, despite problems with interpreting changes in measured total carbonate content of sediments, the CDI contains more information on carbonate loss than indices based on fragmentation alone [*Peterson and Prell*, 1985a]. *Peterson and Prell's* [1985a] CDI is not only a useful measure of preservation but is also applicable for downcore studies where multiple preservation indices can be represented by a single variable [*Peterson and Prell*, 1985a].

[12] *Le and Shackleton* [1992] compared three indices of carbonate preservation, BDI, number of whole foraminifera per dry sediment weight [NGS], and the ratio of fragmented to whole foraminifera, in quantifying carbonate dissolution in the western equatorial Pacific. Both BDI and NGS are controlled by ecological factors to some degree; however, correlation between these two indices improves with increasing water depth. This suggests that their ecological bias can be overwritten by dissolution effects with water depth [*Le and Shackleton*, 1992] and that they can be used as reliable indices in samples below the lysocline. However, NGS may also be prone to analytical errors [*Le and Shackleton*, 1992]. Thus, *Le and Shackleton* [1992] found their fragmentation ratio to be the more direct indicator of dissolution when compared to the BDI and NGS.

[13] *Lohmann* [1995] demonstrated that over 50% of the primary shell for *Globigerinoides sacculifer* is dissolved before shell fragmentation begins. This dissolution begins approximately 2000 meters above the foraminiferal lysocline [*Lohmann*, 1995]. Hence, fragmentation occurs along a continuum of the dissolution process and reflects more the middle to terminal stages of calcite loss.

[14] Although a calibration of a fragmentation index with the percent of carbonate dissolved has long been sought [e.g. *Adelseck*, 1978], due to data constraints dissolution indices have been correlated with other dissolution indices or with water depth rather than to the desired variable. We have developed a transfer function that directly relates fragmentation ratios for one planktic foraminiferal species with percent calcite dissolved. Our transfer function is different from previous dissolution indices because we calculate the percent carbonate dissolved through biogeochemical modeling independent of faunal assemblages.

## 2.2. Modeling Calcite Dissolution

[15] The preservation and dissolution of  $\text{CaCO}_3$  in sediments is controlled by a range of processes that must be resolved in a diagenetic model. The dissolution rate is governed by the saturation state, which in seawater is largely controlled by the concentration of the carbonate ion. Carbonate ion, in turn, is tied to the carbonate buffer

species,  $\text{CO}_2$  and  $\text{HCO}_3^-$  by the fast equilibrium pH chemistry of seawater. These reactions link calcite dissolution to other pH-active reactions such as the degradation of organic carbon.

[16] We estimated calcite dissolution rates for sites we studied using the Muds model of pore water pH and redox chemistry [*Archer et al.*, 2002]. The model is driven by sinking fluxes of organic carbon and  $\text{CaCO}_3$  to the seafloor and uses the chemistry of the overlying water as a boundary condition. Dissolution of  $\text{CaCO}_3$  is driven by the undersaturation of the overlying water, and by the products of organic carbon degradation within the near-surface sediment. Given these constraints, the predicted rate of  $\text{CaCO}_3$  dissolution is sensitive to the depth and the metabolic pathway of organic matter degradation. Pore water acidification by oxic carbon degradation, for example, provokes  $\text{CaCO}_3$  dissolution if the reaction occurs a centimeter or more below the sediment surface. Oxic metabolism at the sediment surface is expected to have very little influence on pore water pH or  $\text{CaCO}_3$  dissolution. Degradation by other electron acceptors ( $\text{NO}_3^-$ ,  $\text{MnO}_2$ ,  $\text{FeOOH}$ , and  $\text{SO}_4^{2-}$ ) does not acidify the pore waters, although if the reduced products ( $\text{Mn}^{2+}$ , for example) diffuse to the oxic zone and react with  $\text{O}_2$ , this generates a source of acid.

[17] The model predicts the depths and pathways for organic carbon degradation by solving for the steady state distribution of solid phase and pore water constituents within the top meter of the sediment. Rate constants for bioturbation and carbon degradation are parameterized as a function of the rain rate of organic matter to the seafloor. These empirical parameterizations were extensively tuned to reproduce the concentrations of organic carbon,  $\text{MnO}_2$ ,  $\text{O}_2$ ,  $\text{NO}_3^-$ ,  $\text{Mn}^{2+}$ ,  $\text{Fe}^{2+}$ , and  $\text{NH}_4^+$  in a compilation of sediment cores from the shallow waters to the abyss [*Archer et al.*, 2002]. The dissolution rate of  $\text{CaCO}_3$  in Muds has been ground-truthed to benthic flux data from the California continental slope [*Berelson et al.*, 1996] and to micro-electrode data from the Ceara Rise and the Ontong Java Plateau [*Hales and Emerson*, 1996, 1997a]. *Hales and Emerson* [1997b] argue for a first-order dissolution rate law for  $\text{CaCO}_3$ , and conclude that the dissolution rate constant from Ontong Java is slower than at Ceara Rise by an order of magnitude. On the other hand, laboratory measurements argue for nonlinear dissolution kinetics for  $\text{CaCO}_3$  [*Keir*, 1980]. Our experience (not shown) is analogous to Hales'; we find that using linear dissolution kinetics we are able to reproduce shelf, slope, and abyssal dissolution rate data, whereas with higher-order kinetics we require 1–2 orders of magnitude variability in dissolution rate constant. We therefore chose linear kinetics, using Hales' Ceara Rise rate constant ( $10^{-4} \text{ day}^{-1}$ ) for the simple benefit of generality.

## 3. Transfer Function

[18] Our calibration sample set is made up of 38 samples, 16 of which are from the East Pacific Rise within  $95^\circ\text{W}$ – $110^\circ\text{W}$  and  $5^\circ\text{S}$ – $10^\circ\text{S}$ . The other 22 samples are from the Ontong Java Plateau from  $158^\circ\text{E}$ – $163^\circ\text{E}$  and  $0^\circ$ – $10^\circ\text{S}$ . The water depth for our calibration samples ranges from 1900 to

**Table 1.** Location and Depth Information and Modeling Data for Calibration Samples<sup>a</sup>

Sample Number	Water Depth, m	Latitude	Longitude	Delta Calcite, μmol/kg	Percent Calcite	MFI	Percent Dissolved (Regress MFI)	Percent Dissolved With Muds
KK71 FFC 199	3049	-6.250	-106.620	-13.28	82.00	0.46	52.7	61.9
Y71-9-97GC	3319	-6.600	-106.807	-16.32	88.67	0.58	62.1	67.8
Y71-9-92MG1	3350	-6.800	-106.110	-16.67	83.34	0.54	59.2	67.8
OC73-4-34MG3	3366	-7.280	-107.612	-16.85	88.01	0.64	65.9	68.3
Y71-9-100FF	3386	-6.450	-106.837	-17.08	78.17	0.72	70.1	67.3
Y71-9-99FF	3395	-6.460	-106.813	-17.18	9.76	0.64	65.9	67.8
VNTR01-10GC	3405	-4.510	-102.016	-17.29	77.84	0.74	71.0	67.8
Y71-9-96	3470	-6.640	-106.443	-18.03	84.26	0.66	67.0	69.8
Y71-9-112G	3490	-6.250	-107.277	-18.25	65.92	0.55	59.9	66.3
Y71-9-95FF	3649	-6.720	-106.323	-20.05	75.67	0.89	75.5	70.8
AMPH 25G	3660	-9.050	-105.883	-20.17	85.84	0.81	73.5	73.3
Y71-9-94P	3687	-6.650	-106.288	-20.48	78.42	0.91	75.8	72.3
SCAN 94PG	3900	-7.440	-102.640	-22.88	68.92	0.99	76.5	72.8
Y71-9-89MG3	3990	-5.980	-101.025	-23.89	67.17	0.99	76.5	73.8
Y71-7-35MG1	4010	-9.950	-97.938	-24.12	75.09	0.97	76.4	76.7
CARR 2 4G	4060	-8.867	-103.483	-24.68	91.92	0.96	76.4	80.7
ERDC 110G	3003	-1.738	160.487	-12.76	79.92	0.55	59.9	57.4
ERDC 126G	3328	-0.018	160.983	-16.43	81.92	0.59	62.7	64.1
ERDC 109G	3636	-1.743	160.783	-19.90	77.92	0.79	72.9	68.7
ERDC 127PG	3724	-0.003	161.418	-20.89	78.67	0.83	74.1	70.3
ERDC 130PG	4123	-0.040	161.917	-25.39	79.59	0.83	74.1	76.9
ERDC 132PG	4441	-0.043	162.683	-28.98	67.67	0.97	76.4	77.4
ERDC 91 G	1900	-0.868	157.495	-0.32	74.53	0.23	28.1	32.8
ERDC 101G	2106	-3.243	159.382	-2.64	77.80	0.32	38.8	38.0
ERDC 104G	2255	-3.668	161.295	-4.32	79.30	0.45	51.8	41.5
ERDC 107G	2675	-2.620	161.350	-9.06	79.46	0.46	52.7	50.8
ERDC 117G	2275	-1.033	159.472	-4.55	72.67	0.41	48.1	41.5
ERDC 122G	2542	-0.133	159.523	-7.56	77.41	0.38	45.1	47.7
ERDC 116G	2272	-0.998	159.468	-4.51	79.86	0.42	49.0	42.1
ERDC 114G	2151	-1.637	159.200	-3.15	79.83	0.39	46.1	39.0
ERDC 118G	2163	-0.982	158.800	-3.28	79.95	0.38	45.1	38.5
ERDC 115G	2157	-1.645	159.198	-3.22	81.60	0.38	45.1	39.5
ERDC 90G	1903	-0.865	157.480	-0.35	81.97	0.42	49.0	32.8
ERDC 111G	2667	-1.710	159.917	-8.97	81.80	0.36	43.1	51.3
ERDC 89PG	1932	-0.033	155.865	-0.68	82.90	0.26	31.8	33.9
ERDC 121G	2245	-0.183	158.713	-4.21	80.79	0.33	39.9	41.5
ERDC 98G	1977	-2.833	158.473	-1.19	83.03	0.37	44.1	34.9
ERDC 119G	2148	-0.990	158.600	-3.12	100.00	0.28	34.2	38.0

<sup>a</sup> Percent dissolved from Muds using organic carbon and calcite fluxes derived as explained in the text.

4441 m (Table 1). These samples are from surface sediments of gravity cores so as to reflect oceanographic conditions integrated over the recent past. We interpret our coretop samples as recent based on their physical characteristics (reflecting the surficial oxic, upper 1- to 2-cm zone of the sediments) and previously published work [Loubere, 1994] showing a strong correlation between their benthic foraminiferal assemblages and modern surface ocean biological productivity (this for the EPR area). We elected to examine calcite preservation using the foraminiferal species *G. menardii* as an index because previous work [Ku and Oba, 1978] suggested that fragmentation in this taxon might be linear to dissolution.

### 3.1. Data for Modeling

[19] Data used in deriving our transfer function are presented in Table 1. The Muds model required input of bottom water oxygen content, nitrate, silica, alkalinity, delta calcite (difference between saturation and in situ carbonate ion concentration), water depth, organic carbon flux, and percent calcite in the sediments in order to calculate calcite dissolution flux for each of our calibration locations. We then used the following equation to calculate percent calcite

dissolved for each sample: % calcite dissolved = (dissolution rate/calcite flux) × 100.

[20] We extrapolated chemical data for each of our samples using a gridded global field [e.g., Archer, 1996b]. The calculation of delta calcite values is detailed by Archer [1996a, p. 514]. Sediment calcite content was measured directly on our samples using an NA-1500 C/N/O/S analyzer and the methods of Verardo *et al.* [1990]. The analytical error was ±2.4% with respect to pure carbonate standards.

[21] We used uniform regional organic flux values for the Ontong Java Plateau and the East Pacific Rise derived from the surface ocean productivity compilations of Berger *et al.* [1987], Berger [1989], and Behrenfeld and Falkowski [1997] and the water depth relationship of Berger *et al.* [1987]. These sources yield organic carbon fluxes for the Ontong-Java area ranging from 7.8 to 11.8 μmol/cm<sup>2</sup>/yr and averaging 10 μmol/cm<sup>2</sup>/yr; for the EPR area the range was 10.5 to 14.3 μmol/cm<sup>2</sup>/yr with an average of 12 μmol/cm<sup>2</sup>/yr.

[22] Calcite flux values for specific locations are more uncertain due to scarcity of data as outlined by Archer [1996a]. Therefore, we estimated calcite flux using averaged calcite accumulation and dissolution rates (calcite flux =

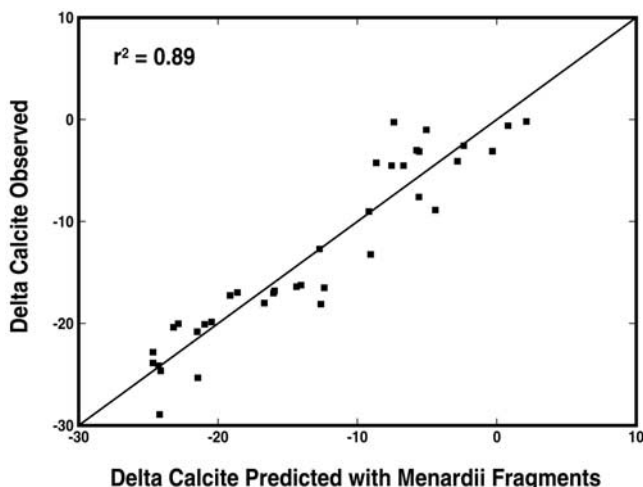


**Figure 1.** Regression of observed delta calcite values ( $\mu\text{mol/kg}$ ) from Archer's [1996a] database versus delta calcite values calculated by our *G. menardii* fragmentation index.

dissolution flux + accumulation rate) at our two calibration locations. In the case of the Ontong Java plateau, Berger and Killingley [1982] provide data which allow calculation of accumulation rates between 6 and 14  $\mu\text{mol/cm}^2/\text{yr}$  for water depths around 2500 m. Our modeling finds dissolution rates of 9 to 10  $\mu\text{mol/cm}^2/\text{yr}$  for these water depths which gives a calcite flux between 15 and 24  $\mu\text{mol/cm}^2/\text{yr}$ . This yields an organic carbon to calcite flux ratio of 0.42–0.67; on average, 0.55. This ratio value is what we would expect from Archer's [1996a] data-driven model results for the western equatorial Pacific (his Figure 7). For the EPR calibration area, we calculated calcite accumulation rate data from information from McMurtry *et al.* [1981]. Here a number of cores close to our sampling locations yield calcite accumulation rates that average to 7.1  $\mu\text{mol/cm}^2/\text{yr}$  for water depths between 3000 and 3350 m. For these water depths, the Muds dissolution rates are between 12.5 and 13.7  $\mu\text{mol/cm}^2/\text{yr}$ , producing an estimated average calcite flux of 19.6–20.8  $\mu\text{mol/cm}^2/\text{yr}$ . In this case the organic carbon to calcite flux ratio using our figures is 0.6 (0.58–0.61), which corresponds to that expected from Archer [1996a].

[23] Since a reasonable range for the organic carbon to calcite flux ratio for our locations appears to lie between 0.5 and 0.6, the range in our possible estimates of the calcite flux yields an uncertainty in our calculated percent dissolved of about 10%. For the purposes of modeling below we use the average numbers listed above. The percent dissolved we calculated for our calibration areas is listed in Table 1.

### 3.2. *Globorotalia menardii* Fragmentation Index (MFI)

[24] Our index is based on counting fragments of *Globorotalia menardii* specimens. We chose this species above all others because (1) it is very easy to identify even by a nonspecialist, (2) it shows progressive fragmentation with increased undersaturation of the carbonate ion in seawater [Ku and Oba, 1978] unlike other species which remain intact

until very high degrees of undersaturation and then suddenly fall to pieces, and (3) its fragments, regardless of degree of dissolution, are easy to identify and do not allow for confusion with other species. We defined four categories of *G. menardii* fragments which are then combined in an equation: (a) whole, completely intact, undamaged specimens, (b) specimens with small holes or where more than half of the individual is intact, (c) specimens where less than half of the individual is intact, and (d) fragments of keels only. Using these categories we calculate our index for each sample with the following equations:  $D = \#$  of damaged specimens;  $D = [b + (c/3) + (d/5)]$ ; and  $\text{MFI} = D/(D + \# \text{ in } a)$ . We used the 1/3 and 1/5 fractions in categories c and d to represent the average value for the number of fragments that would be produced by the dissolution of single intact specimens.

### 3.3. Calibration Equation

[25] To derive our calibration equation, we performed a multivariate linear regression analysis between (1) delta calcite values and our fragmentation index value and its square for each sample and (2) modeled percent calcite dissolved values and our fragmentation index value and its square for each sample. Figure 1 illustrates the relationship between measured delta calcite values and those predicted by our *G. menardii* fragmentation index. The  $R^2$  is 0.89, and the average prediction error is  $\pm 2.29 \mu\text{mol/kg}$ . Figure 2 illustrates the relationship between modeled percent calcite dissolved values and those predicted by our *G. menardii* fragmentation index. The  $R^2$  is 0.88, and the average prediction error is  $\pm 5.8\%$  dissolved. Our results show that the *G. menardii*-based index has a consistent relationship to the proportion of the calcite flux being dissolved at the seabed. A precise determination of that relationship is limited by uncertainties for the calcite and organic carbon fluxes as well as by modeling uncertainties, but the index will reflect both the direction and relative magnitude of changes in percent calcite dissolved. Our

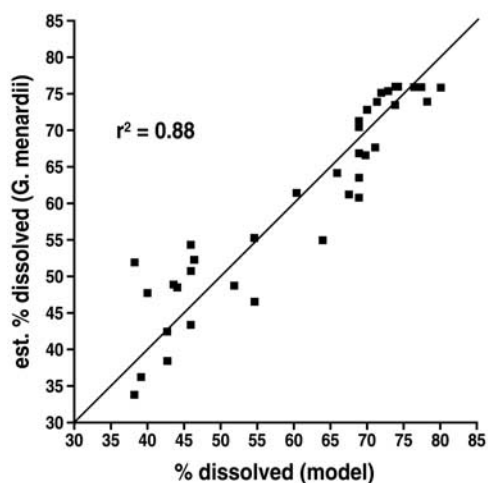


**Figure 2.** Regression of modeled percent calcite dissolved values versus percent dissolved values calculated by our *G. menardii* fragmentation index (equation in text).

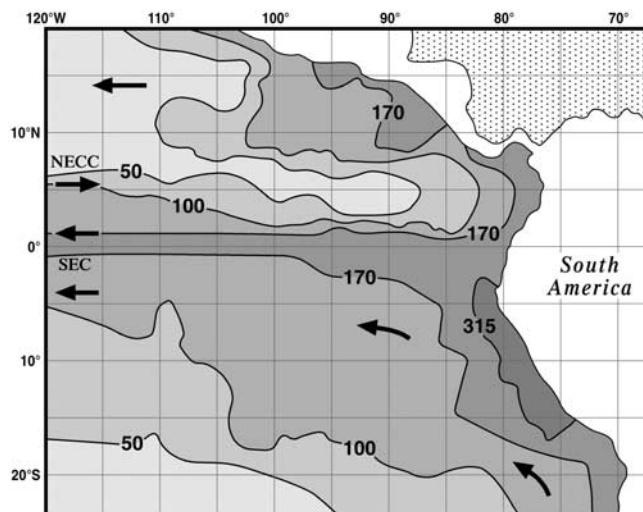


**Figure 3.** Surface ocean productivity map for the eastern equatorial Pacific [after Behrenfeld and Falkowski, 1997]. Units in  $\text{gC}/\text{m}^2/\text{yr}$ . NECC = North Equatorial Countercurrent, SEC = South Equatorial Current.

calibration equation is percent calcite dissolved =  $-5.111 + (\text{MFI} \times 160.491) - (\text{MFI}^2 \times 79.636)$ .

#### 4. Organic Carbon Flux, the Organic C/Calcite Flux Ratio, and Calcite Preservation

[26] A classic problem in the study of the deep-sea carbonate record is the determination of the degree to which that record reflects organic carbon flux to the seabed, as well as degree of bottom water calcite saturation. Our calibration was done specifically avoiding large variations in organic carbon flux so as to minimize uncertainties in estimating percent of the calcite flux which dissolved at the seafloor. This was done by selecting closely grouped surface sediment samples within limited geographic areas (Table 1). However, we can test for the impact of changing organic carbon flux, and changing organic carbon to calcite flux ratio, by applying our index to a region where there are strong gradients in fluxes and ratio. The eastern equatorial Pacific is such a place.

[27] The eastern equatorial Pacific (EEP) is a classic area for oceanographic studies as (1) it hosts a significant portion of global biological productivity (about 18–56% of global new production [Chavez and Barber, 1987]); (2) it is an important region of carbon dioxide evasion into the atmosphere [Tans et al., 1990] driven by a dynamic balance between surface water properties and biologic productivity [Murray et al., 1994]; and (3) it plays a notable role in the global nitrogen budget [Codispoti and Christensen, 1985; Toggweiler et al., 1991]. These unique regional properties result mainly from shallow equatorial upwelling and from deeper upwelling along the coast of Peru which brings waters originating from the subantarctic to the surface [Toggweiler et al., 1991]. The zones of highest productivity are generally along Peru [Suess and Thiede, 1981] and the equator. This is shown in Figure 3.

[28] The strong regional productivity gradients across the EEP afford us the opportunity to differentiate the effects of deep-water calcite saturation and organic carbon flux on our calcite preservation index. Also, a synthesis of sediment trap data [Archer, 1996a] shows that there is strong variation in the organic carbon/calcite flux ratio across the EEP, presumably reflecting changes from diatom dominated phytoplankton communities off Peru to those with mostly picoplankton and coccolithophores farther to the west and south [e.g., Landry et al., 1996]. We test the variability of this ratio in the EEP for 46 core top samples (see Tables 2 and 3 and Figure 4; this does not include any samples used in the EPR calibration) from this region for which we estimated the percent calcite dissolved both by biogeochemical modeling and our *G. menardii* fragmentation index.

[29] Figure 5 illustrates the regional pattern of percent calcite dissolved in the EEP calculated by our calibration equation. All data used in the application of our transfer function to EEP samples are listed in Tables 2 and 3. In Figure 5, the imprint of the North Equatorial Countercurrent and the Peru Current are discernable (compare with NECC and SEC in Figure 3) as there is a clear gradient of increasing calcite dissolution toward South America in the equatorial band and along the coast. We now need to compare these results with modeled values for percent calcite dissolved in this region in order to determine the contribution of seabed organic carbon oxidation to calcite dissolution.

[30] Figures 6a and 6b show theoretical percent calcite dissolved values for EEP samples calculated by biogeochemical modeling alone. We obtained values for delta calcite for each sample location from Archer's [1996a] global gridded field database. We obtained values for each sample location for organic carbon flux from Jahnkes [1996] global gridded database for oxygen consumption rates using an  $\text{O}_2/\text{CO}_2$  ratio of 138/106 [Redfield, 1934; Redfield et al., 1963; Richards, 1965] and 154/106 [Anderson, 1995; Hedges et al., 2002] and from surface ocean productivity data [Berger et al., 1987; Berger, 1989; Behrenfeld and Falkowski, 1997] with the water depth relationship of Berger et al. [1987] (Table 3). The modified Redfield ratio is taken as an improved representation of biogeochemical reactions at the seabed. All the organic carbon flux estimators share a common pattern across the EEP; we found that the correlation between the surface ocean productivity and oxygen-flux-based (154/106) estimates was 0.89. For illustration purposes we used the productivity-based estimates, or show results averaged for all three estimators.

[31] In Figure 6a, we calculated percent calcite dissolved by using a constant organic carbon flux value and a constant organic carbon flux to calcite flux ratio for modeling purposes ( $12 \mu\text{mol}/\text{cm}^2/\text{yr}$  and 0.6, respectively: the same values used for calibration samples from the East Pacific Rise). Thus, Figure 6a shows a pattern of calcite dissolution in the EEP assuming that bottom water calcite undersaturation is the only controlling factor on calcite dissolution, as both organic carbon flux and the ratio are being kept constant across the region, at values we used for calibrating our index.

**Table 2.** Data Used for Application of Calibration Equation and Muds Model to Eastern Equatorial Pacific Samples

Sample Number in Figure 4	Latitude, deg	Longitude, deg	Water Depth, m	Delta Calcite, $\mu\text{mol/kg}$	Percent Calcite	MFI
1 V69-86-M2	1.978S	91.667W	3245	-15.56	40.82	1.00
2 VNTR 01-11GC	7.86N	95.340W	3345	-15.79	52.14	0.89
3 BNFC 25PG	10.357N	108.107W	2693	-7.52	84.80	0.95
4 Y-71-3-5 FF5	5.92N	84.938W	2363	-9.92	35.66	0.95
5 W 7706-69	4.2S	85.34W	3537	-16.50	52.67	0.96
6 VLCN I 26 GC	8.797N	103.992W	3099	-7.94	27.26	0.95
7 Y69-110 M	0.21S	81.093W	3083	-15.78	47.56	0.72
8 BNFC 39G	10.12N	109.045W	3041	-7.99	67.15	0.98
9 VLCN I 18GC	8.793N	103.992W	3082	-7.70	34.13	0.99
10 P6702-9	2.067S	103W	3281	-14.13	83.71	0.74
11 Y71-3-4MG5	5.802N	84.963W	2628	-11.08	28.04	0.78
12 Y71-3-3MG3	7.050N	85.5W	2551	-13.41	18.88	0.85
13 Y71-3-11 MG1	0.28S	83.275W	2656	-9.73	45.95	0.67
14 Y71-6-12 MG	16.443S	77.563W	2734	-0.42	26.82	0.83
15 GS7202-17	2.3S	97.933W	3371	-16.05	68.74	0.85
16 AII 54 14PG	5.732S	107.568W	3190	-9.14	76.00	0.36
17 KK7 FFC188W	5.97S	106.903W	2954	-8.23	76.00	0.51
18 BNFC 44PG	10.49N	109.023W	2845	-12.14	85.60	0.84
19 AMPH-19G	8.333S	107.783W	3090	-9.87	84.52	0.42
20 GS 7202-15	3.267N	97.833W	2986	-12.39	53.43	0.61
21 Y71-3-15	1.465S	85.692W	2660	-13.81	75.62	0.81
22 GS 7202-16	0.067N	98.533W	3183	-13.14	65.00	0.83
23 P6702-57	1.33N	87.183W	2749	-16.82	46.00	0.75
24 AII 54 1GC	7.433S	108.25W	3170	-7.83	76.00	0.48
25 Y71-9-104	6.092S	107.077W	2988	-9.19	75.94	0.63
26 AMPH 31 GV	18.467S	112.183W	3160	-6.66	85.09	0.38
27 GS 7202-33 FC	12.158S	112.4W	3119	-7.53	81.54	0.22
28 P6702-59	2.75N	85.33W	3274	-20.77	62.84	0.84
29 Y69-103M2	0.08N	82.427W	1808	-3.46	97.76	0.81
30 Y69-106M2	2.98N	86.557W	2870	-13.83	48.88	0.99
31 KK74-01-09FFC-7	0.49N	102.177W	3100	-6.82	65.00	0.72
32 Y-69-80 M2	1.02S	91.985W	3408	-18.02	55.86	0.92
33 PLDS 4 G	3.433S	102.703W	3194	-13.09	77.50	0.80
34 AII 54 14PC	5.732S	107.568W	3190	-9.14	76.00	0.46
35 Y71-3-13 MG1	1.8S	85.81W	2798	-15.72	6.81	0.62
36 Y71-9-115	6.267S	107.237W	3139	-8.11	70.22	0.53
37 P 6702-35G	8.317S	109.85W	2914	-6.07	78.90	0.43
38 Y71-3-19 FF1	1.9S	82.25W	2580	-12.72	67.99	0.68
39 P 6702-33G	10.017S	109.65W	3124	-7.98	78.57	0.32
40 OC 73-3-24P	20.205S	112.112W	3254	-11.48	62.84	0.32
41 P6702-1	5N	103W	3159	-10.85	77.36	0.66
42 Y71-3-15	1.465S	85.692W	2660	-13.81	75.62	0.70
43 Y71-7-45P	11.083S	110.103W	3096	-7.49	80.44	0.27
44 KK74-01-09FFC-5	0.481N	102.138W	2947	-11.61	52.00	0.59
45 KK 71 FFC 205	6.1S	106.59W	2948	-8.93	76.00	0.53
46 KK 74 FFC 7	0.490N	102.177W	3100	-6.88	84.00	0.70

[32] In Figure 6b we did another experiment assuming that the organic carbon to calcite flux ratio is uniform across the region (0.6) but using different organic carbon flux numbers for each sample which we acquired as described above.

[33] Comparing Figures 6a and 6b reveals significantly different patterns with percent dissolved generally lower in the model having a variable organic carbon flux (Figure 6b). It is worth noting that when the organic carbon flux to calcite flux ratio is kept constant, an increase in organic carbon flux does not necessarily produce an increase in calcite dissolution. The central equatorial region has percent calcite dissolved over 60 in Figure 6a whereas this area shows only 45–50% dissolution in Figure 6b, although the organic carbon flux values used for these samples were significantly higher in Figure 6b. The cause for this counter-intuitive result lies in a higher calcite flux value needed for samples in Figure 6b in order to keep the flux ratio constant.

The higher calcite flux promotes calcite preservation and counters the effects of corrosive bottom water, which has a larger effect in Figure 6a. Figure 7 illustrates the above point by comparing selected sites under the two modeling conditions.

[34] Neither Figure 6a nor 6b resembles our *G. menardii*-based percent calcite dissolved map in Figure 5. Figure 6c illustrates the difference between values in Figures 5 and 6a, and Figure 6d illustrates the difference between Figures 5 and 6b. The results in Figures 6a and 6c demonstrate that calcite undersaturation in bottom waters alone is not sufficient to account for the dissolution recorded by the foraminifera. Figure 6c shows a regionally coherent pattern with the greatest positive differences between the foraminiferal index and the model occurring in areas with higher bio-productivity (see Figure 3). Negative differences are found where productivity is lower.

**Table 3.** Data Used for Application of Calibration Equation and Muds Model to Eastern Equatorial Pacific Samples<sup>a</sup>

Sample Number in Figure 4	Organic C Flux 1 138/106	Organic C Flux 2 154/106	Organic C Flux 3 Production	<i>Menardii</i> % Dissolved	Rain Ratio 1	Rain Ratio 2	Rain Ratio 3	Constant Organic C % Dissolution	Variable Organic C % Dissolution
1	22.28	19.96	22.86	75.7	1.05	1.00	1.07	56.5	42.5
2	22.28	19.96	15.08	74.7	0.98	0.94	0.83	60.0	53.7
3	11.52	10.32	13.59	75.5	0.85	0.81	0.91	52.5	49.9
4	30.72	27.53	25.79	75.5	1.34	1.27	1.24	49.0	36.5
5	30.72	27.53	29.61	75.5	1.13	1.07	1.10	60.5	41.1
6	16.13	14.45	16.13	75.5	1.18	1.14	1.18	42.5	38.3
7	53.77	48.18	31.03	69.2	1.42	1.32	1.06	60.0	39.1
8	11.52	10.32	12.99	75.7	0.88	0.84	0.92	51.0	49.4
9	16.13	14.45	16.16	75.7	1.14	1.09	1.14	44.0	39.7
10	22.28	19.96	18.98	70.1	0.87	0.83	0.81	63.5	51.8
11	30.72	27.53	24.70	71.7	1.33	1.25	1.21	47.5	35.5
12	34.57	30.97	30.55	73.8	1.58	1.49	1.47	45.5	30.1
13	53.77	48.18	30.07	66.7	1.48	1.38	1.11	51.0	36.1
14	34.57	30.97	33.79	73.3	1.72	1.66	1.71	33.5	25.8
15	22.28	19.96	18.80	73.8	0.91	0.87	0.85	64.5	52.3
16	22.28	19.96	15.97	42.2	0.59	0.57	0.53	53.5	48.1
17	22.28	19.96	16.41	56.0	0.79	0.77	0.72	52.5	46.8
18	11.52	10.32	13.31	73.6	0.70	0.67	0.75	61.5	58.6
19	22.28	19.96	11.63	48.2	0.65	0.62	0.51	56.0	56.8
20	22.28	19.96	14.39	63.2	0.87	0.84	0.73	56.0	51.7
21	42.25	37.86	32.78	72.7	1.17	1.12	1.05	64.0	41.4
22	22.28	19.96	23.01	73.3	0.97	0.92	0.98	59.0	44.9
23	34.57	30.97	20.23	70.5	1.12	1.06	0.87	62.0	48.6
24	16.13	14.45	11.52	53.6	0.70	0.67	0.62	51.5	52.1
25	22.28	19.96	16.34	64.5	0.90	0.86	0.80	54.0	48.1
26	7.68	6.88	5.13	44.3	0.45	0.43	0.38	50.0	69.0
27	16.13	14.45	7.73	26.0	0.34	0.32	0.25	51.5	61.3
28	34.57	30.97	13.93	73.6	1.04	0.98	0.67	72.0	66.3
29	53.77	48.18	38.81	72.7	1.57	1.50	1.40	43.5	31.1
30	34.57	30.97	29.19	75.7	1.25	1.18	1.14	57.5	39.7
31	22.28	19.96	19.35	69.2	1.04	1.01	1.00	48.5	41.6
32	30.72	27.53	19.98	75.1	1.07	1.01	0.89	64.5	50.5
33	22.28	19.96	17.88	72.4	0.92	0.88	0.85	61.0	51.3
34	22.28	19.96	15.97	51.8	0.73	0.70	0.65	53.5	48.1
35	42.25	37.86	32.15	63.8	1.00	0.96	0.89	68.0	43.1
36	22.28	19.86	16.06	57.6	0.83	0.80	75.00	51.5	46.0
37	11.52	10.32	11.88	49.1	0.60	0.57	0.60	48.5	49.0
38	42.25	37.86	33.18	67.3	1.12	1.07	1.02	61.0	39.6
39	11.52	10.32	11.58	37.9	0.43	0.41	0.43	52.0	52.9
40	4.61	4.13	3.81	37.9	0.26	0.24	0.23	56.0	99.2
41	16.13	14.45	14.10	66.2	0.79	0.75	0.75	57.0	53.2
42	42.25	37.86	32.78	68.3	1.10	1.05	0.99	64.5	41.4
43	9.22	8.26	7.75	32.2	0.34	0.32	0.32	51.5	61.2
44	26.88	24.09	18.40	61.9	0.93	0.90	0.81	54.5	46.0
45	22.28	19.96	16.42	57.6	0.80	0.77	0.73	54.0	47.5
46	22.28	19.96	20.65	68.3	0.99	0.96	0.97	50.5	42.1

<sup>a</sup>We calculated organic carbon flux in three ways: Organic C flux 1 uses *Jahnke's* [1996] oxygen flux data and a Redfield ratio of 138/106; organic C flux 2 uses *Jahnke's* [1996] data and a Redfield ratio of 154/106; organic C flux 3 uses surface ocean productivity data and water depth relationship to calculate organic carbon flux [Berger et al., 1987; Berger, 1989]. *Menardii* % dissolved is the transfer function estimate. Rain ratio is the organic C to calcite flux ratio calculated with the *menardii* index. Rain ratios are calculated using the respective organic carbon flux 1, 2, and 3 values. Constant organic C % dissolution is the percent dissolved with constant organic C flux and flux ratio. Variable organic C % dissolution is the percent dissolved with variable organic C but with constant flux ratio (this applies to Figure 6; see text).

[35] Figure 6d also shows regionally consistent gradients with highest differences occurring, again, in regions of higher biological productivity (see Figure 3). Difference values are lowest where productivity is low, for example there is a distinct area of low values beneath the North Equatorial Countercurrent (NECC; see Figure 3) which contrasts with higher difference values beneath the equatorial upwelling band.

[36] These data show that incorporating both bottom water undersaturation and organic carbon flux into the model are still not sufficient to account for the dissolution revealed by the foraminiferal index, and that the mismatch

is due to some factor associated with surface ocean bio-productivity. This factor must be the ratio of the organic carbon to calcite fluxes.

## 5. Mapping the Organic Carbon to Calcite Flux Ratio

[37] Since we modeled percent calcite dissolved (Figure 6b) assuming variable organic carbon flux but a constant organic carbon/calcite flux ratio across the EEP, the differences we found in Figure 6d must reflect regional variations in the flux ratio. To test this idea, we calculated an organic carbon to



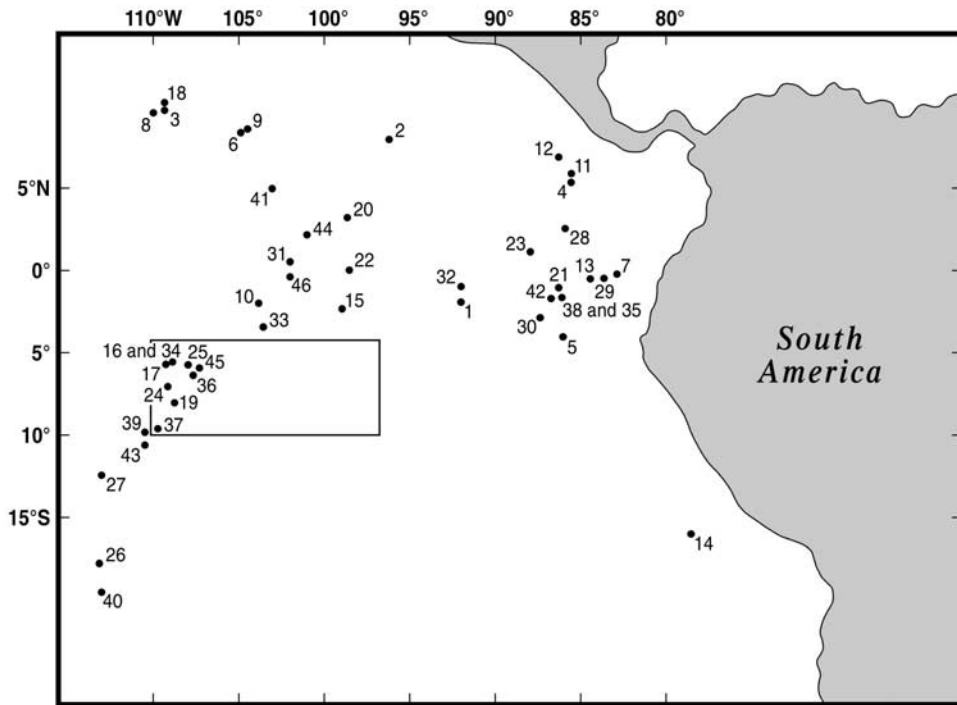


**Figure 4.** Sample location map for 46 surface sediment samples from the eastern equatorial Pacific. See Tables 2 and 3 for data listing. Rectangle shows location of calibration samples along the flank of the East Pacific Rise.

calcite flux ratio for the region using our fragmentation index values. We did this using the following equation (per sample): calcite flux = model-derived calcite dissolution rate/ $G. menardii$ -based fraction calcite dissolved.

[38] Dividing organic carbon flux values for each sample by the calcite flux numbers calculated using the equation above gives us an estimate of the organic carbon to calcite flux ratio for each sample. Results for our three organic

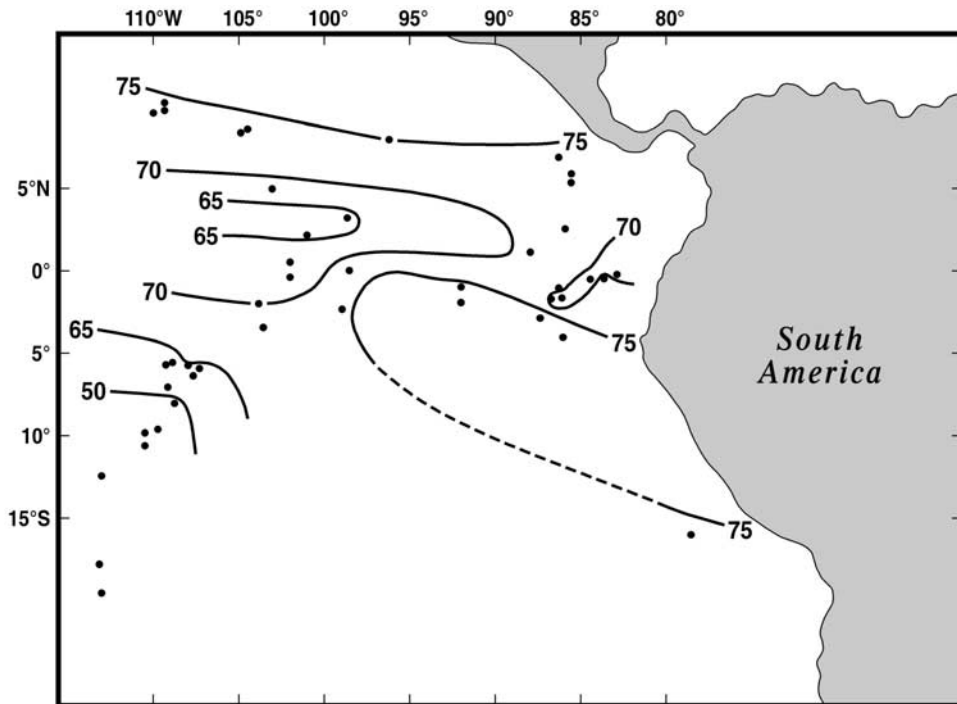


**Figure 5.** Contour map for percent calcite dissolved in the eastern equatorial Pacific calculated by our calibration equation.

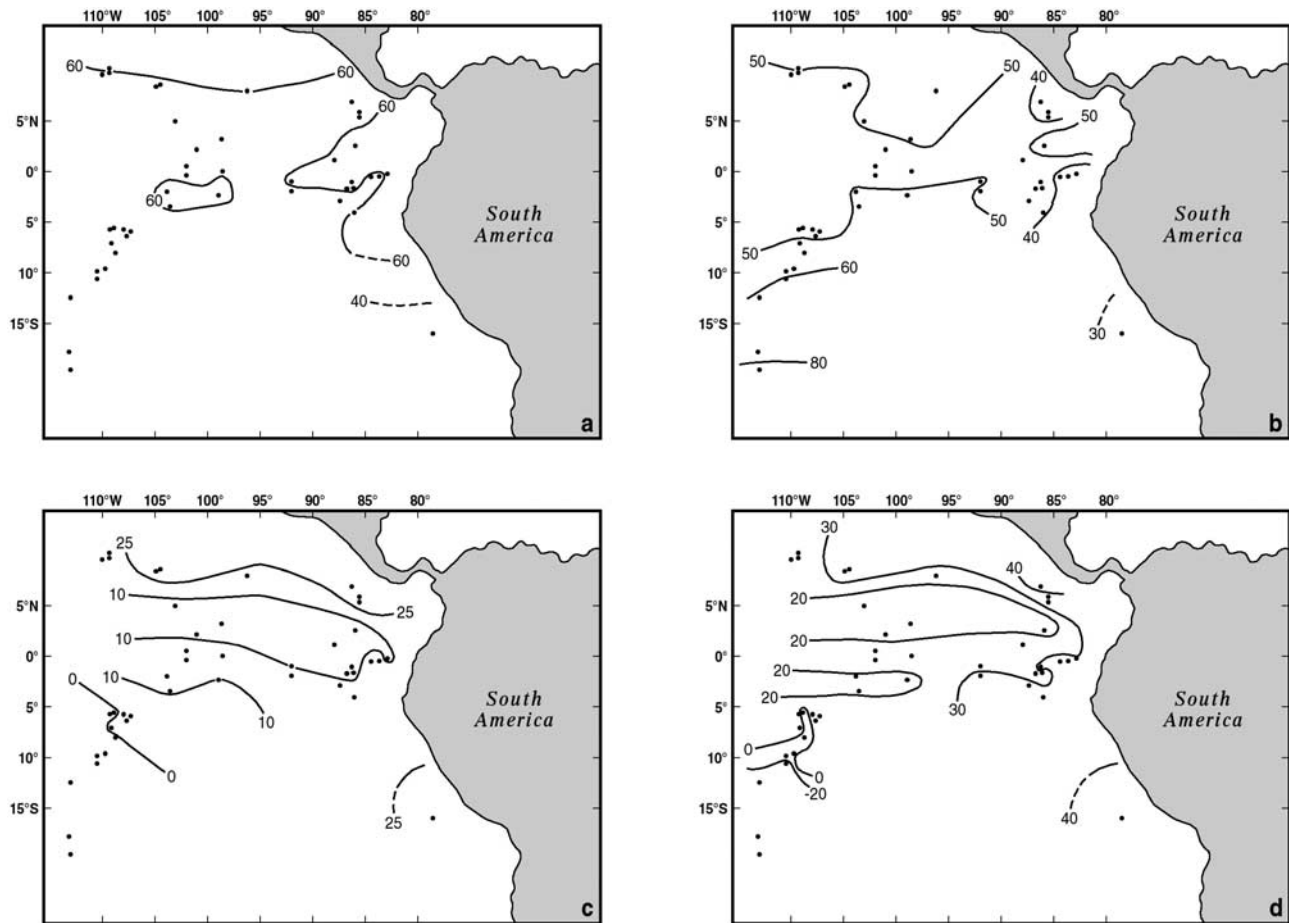


**Figure 6.** Modeled percent calcite dissolved in the eastern equatorial Pacific. (a) Percent calcite dissolved with constant organic carbon flux ( $12 \mu\text{mol}/\text{cm}^2 \text{ yr}$ ) and constant flux ratio (0.6). Calcite saturation is from Archer [1996a]. (b) Percent calcite dissolved with variable organic carbon flux (see Table 3) and constant flux ratio (0.6). Calcite saturation is from Archer [1996a]. (c) Difference between values in Figures 6a and 5. Modeled values in Figure 6a are subtracted from the *menardii*-based percent dissolved values in Figure 5. (d) Difference in values between Figures 6b and 5. Modeled values in Figure 6b are subtracted from the *menardii*-based percent dissolved values in Figure 5.

carbon flux estimators are quite similar and are illustrated in Figure 8, where the contouring takes the three estimates for each location into account (see Table 3 for rain ratios derived from all three estimates of organic carbon flux). The estimates of rain ratio values depend on our initial modeling assumptions; nevertheless, there is clearly a trend in the organic carbon to calcite flux ratio values in Figure 8 which follows trends in surface ocean productivity observed in Figure 3. The pattern of ratio values is clearly associated with regional productivity gradients with highest ratios where productivity is high. This presumably reflects the regional shift to diatom dominated phytoplankton communities where upwelling is strongest. The diatom communities would have relatively lower calcite production and higher  $f$ -ratios (so more organic carbon escapes the photic zone) [Archer, 1996a, Figure 7]. Our estimates of the ratio are compatible with those found along the equator in sediment trap studies and summarized by Archer [1996a] and indicate a three-fold change in the ratio from lowest (southwestern portion of Figure 8) to highest productivity regions.

[39] We conclude that not only the degree of bottom water undersaturation, but also the flux of organic carbon and the organic carbon to calcite flux ratio are incorporated in the deep-sea carbonate record. Also, regional patterns of the organic carbon/calcite flux ratio can be mapped using the *menardii* fragmentation index as long as estimates of dissolution rates can be made.

## 6. Limitations

[40] Our percent calcite dissolution proxy has several limitations. First, it is intended only for the equatorial Pacific as our calibration areas are limited therein. Further, *G. menardii* has a biogeographic range limited to lower latitudes [Bé et al., 1975] and is even completely absent in the Atlantic during some glacials. The ease of identifying even the smallest *G. menardii* fragments and its linear and distinctive fragmentation trend with increasing calcite undersaturation, however, make it ideal as a tool for quantifying fragmentation.

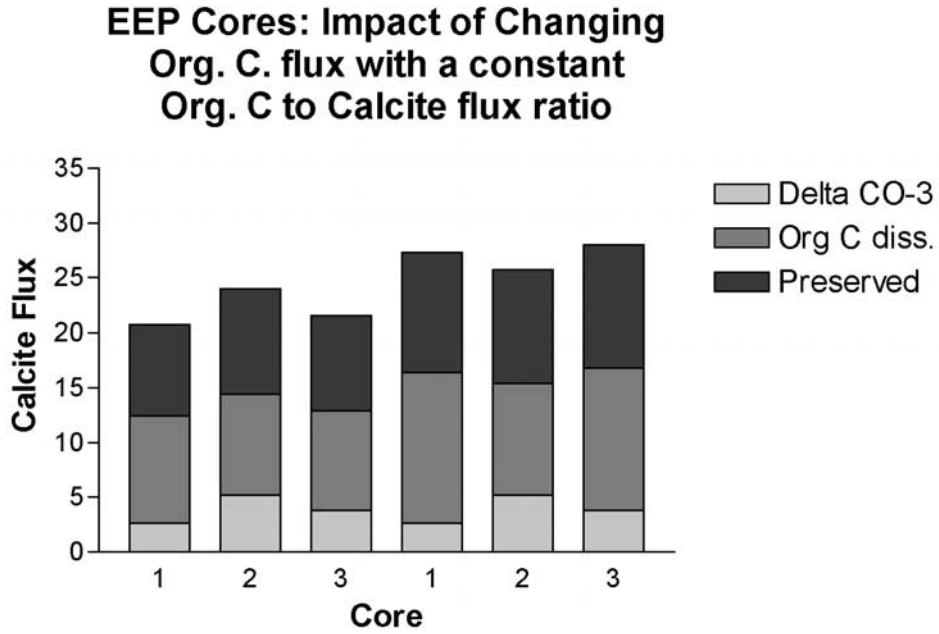


**Figure 7.** Bar graph illustrating differing degrees of calcite preservation with varying organic carbon flux and a constant organic C to calcite flux ratio (0.6). 1 = sample 23, 2 = sample 28, and 3 = sample 32 from Tables 2 and 3. Units are in  $\mu\text{mol}/\text{cm}^2/\text{yr}$ . Samples 1–3 on the left apply to Figure 6a and have an organic carbon flux equal to that of the EPR calibration site. On the right are the same three samples but with organic carbon fluxes taken from the surface ocean productivity synthesis (Figure 6b). From bottom to top the bars show fraction of calcite flux dissolved by bottom water undersaturation (model result neglecting organic carbon rain), fraction dissolved by organic carbon oxidation, and fraction of the calcite flux that is preserved in the sediments.

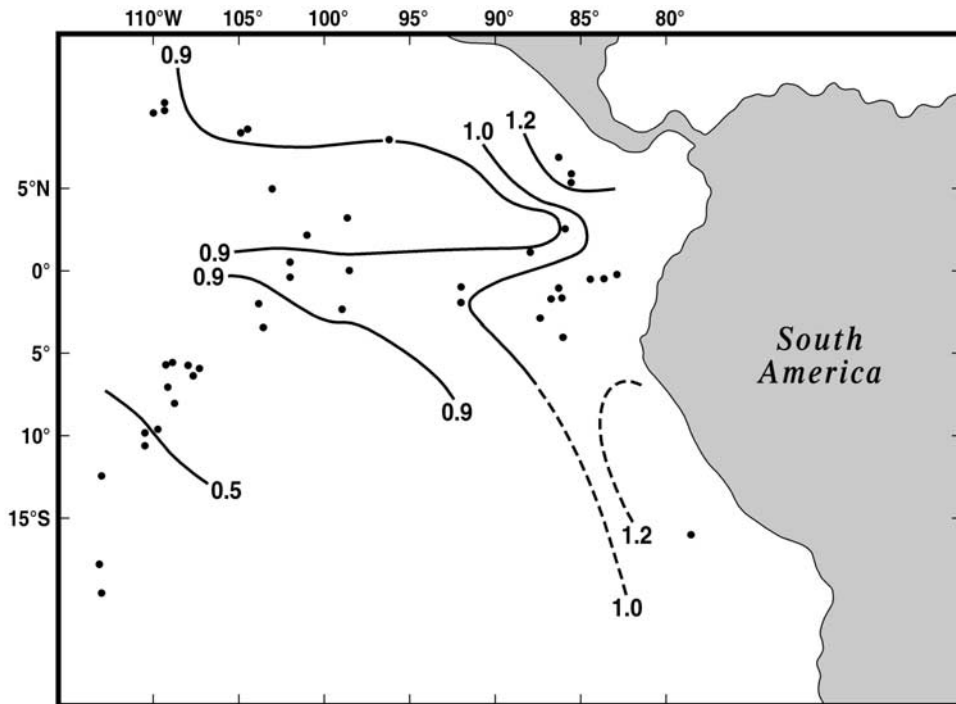


**Figure 8.** Contour map of the organic carbon flux to calcite flux ratio (both units in  $\mu\text{mol}/\text{cm}^2 \text{ yr}$ ) in the eastern equatorial Pacific calculated using our *G. menardii* fragmentation index.

**Table 4.** Sediment Carbonate Data, Core Locations in Table 2

		Water Depth, m	Total % Calcite	% Calcite in >63 $\mu\text{m}$	Fraction of Calcite >63 $\mu\text{m}$
1	Y71-3-5 FF5	2363	44.15	74.48	0.23
2	OC73-3-24P	3254	95.24	100.21	0.44
3	Y71-3-19 MG3	2580	79.87	90.25	0.51
4	P6702-59P	3274	50.20	96.93	0.15
5	Y69-110 M1	3083	61.42	90.56	0.51
6	Y71-3-3MG3	2551	27.16	55.27	0.10
7	Y71-3-13MG2	2798	73.19	96.63	0.27
8	Y71-9-115FF	3139	75.87	87.01	0.42
9	Y69-106M2	2870	65.12	84.55	0.34
10	Y69-80M2	3408	37.59	37.17	0.11
11	Y71-7-45 MG1	3096	86.69	96.12	0.49
12	GS7202-33TW	3119	84.76	95.62	0.52
13	P6702-35G	2914	84.93	95.54	0.43
14	Y71-3-15MG2	2660	88.33	99.13	0.48
15	W7706-69	3537	57.39	86.94	0.22
16	BNFC 39G	3041	75.37	80.62	0.63
17	GS 7202-17TW	3371	71.76	91.78	0.16
18	Y69-103M2	1808	57.75	94.90	0.33
19	Y71-9-104 FF	2988	79.80	94.69	0.44
20	BNFC25PG	2693	91.79	96.14	0.56
21	PLDS4G	3194	81.49	90.77	0.45
22	AMPH19G	3090	87.25	95.03	0.54
23	AMPH31GV	3160	92.90	96.82	0.76
24	V69-86M2	3245	51.79	72.58	0.14
25	GS7202-15TW	2986	87.47	96.47	0.56
26	Y71-3-11MG1	2656	54.73	84.77	0.26
27	Y71-3-4MG5	2628	38.04	85.54	0.17
28	VNTR01-GC11	3345	59.88	78.21	0.18

[41] Another limitation is that our proxy has been tested only for undersaturated conditions. *Jahnke et al.* [1994] have extensively documented an as yet unexplained discrepancy between diagenetic models such as Muds and benthic flux chamber measurements of  $\text{CaCO}_3$  dissolution in supersaturated, high- $\text{CaCO}_3$  conditions. In situ pH micro-electrode data from one of Jahnke's sites seem to indicate  $\text{CaCO}_3$  dissolution as predicted [*Hales and Emerson*, 1996], and as yet no one has come up with a detailed mechanism to explain how the expected dissolution could not be occurring. Shell-thickness data [*Lohmann*, 1995; *Broecker and Clark*, 2001a, 2001b], and foram assemblage data [*Anderson and Archer*, 2002] seem to argue for extensive dissolution of foraminiferal shells in supersaturated conditions. Until the Jahnke paradox is resolved, we take it as a cautionary tale for extrapolating these results to supersaturated conditions.

[42] While our calibration equation captures well the trend of percent calcite dissolved in our study areas, it is possible that the equation is off in the absolute values of its estimates. Error in the absolute range of percent dissolved against which our index is calibrated would result from uncertainty in study area organic carbon fluxes and calcite fluxes and also uncertainties in model solutions for dissolution flux. Biogenic rate constants in Muds, representing organic carbon respiration for example or bioturbation, are parameterized as a function of organic carbon rain rate and overlying water oxygen concentration. While these parameterizations capture most of the larger trends in the data, they fail to reproduce every individual location perfectly [*Archer et al.*, 2002]. The possibility exists for a systematic offset between the model predictions of the dissolution fraction and the reality.

[43] Experimentation shows that changing organic carbon flux by 20% results in a change of about 2.7% in the percent calcite dissolved to which we calibrate our index. Changing the calcite flux by 20% causes a shift of 10% in the percent calcite dissolved estimates. Some constraint is put on the size of the error by the organic carbon to calcite flux ratios which we calculated for the eastern equatorial Pacific (Figure 8). These fall in the ranges expected for the equatorial band on the basis of sediment trap results [*Archer*, 1996a; *Milliman*, 1993], which would not happen if our index were seriously miscalibrated (our ratio values are based on calcite flux calculated by division of model dissolution rates with index estimated fraction of calcite dissolved). This suggests that calcite fluxes used in our calibration are reasonable estimates of true values.

[44] Another potential limitation with sedimentary indices of calcite dissolution or deep-sea carbonate ion concentration is the effect of spatial and temporal variations in sediment properties, such as carbonate content and grain size changes which could potentially influence the amount of calcite dissolution and related foraminiferal fragmentation. For example, *Broecker and Clark* [1999] developed a  $\text{CaCO}_3$  size index as a proxy for measuring the deep-sea carbonate ion concentration in surface and downcore sediments. They acknowledged in a subsequent publication [*Broecker and Clark*, 2001a] that their proxy is sensitive to changes in the source supply of different size fractions of calcite particles. *Broecker and Clark* [2001a] state in their conclusions that eliminating the problem related to the coccolith-rich versus foraminifer-rich fraction of calcareous sediments can either be done by a labor intensive procedure of counting shell fragments and whole shells or by *Lohmann's* [1995] shell weight method. We illustrate here that

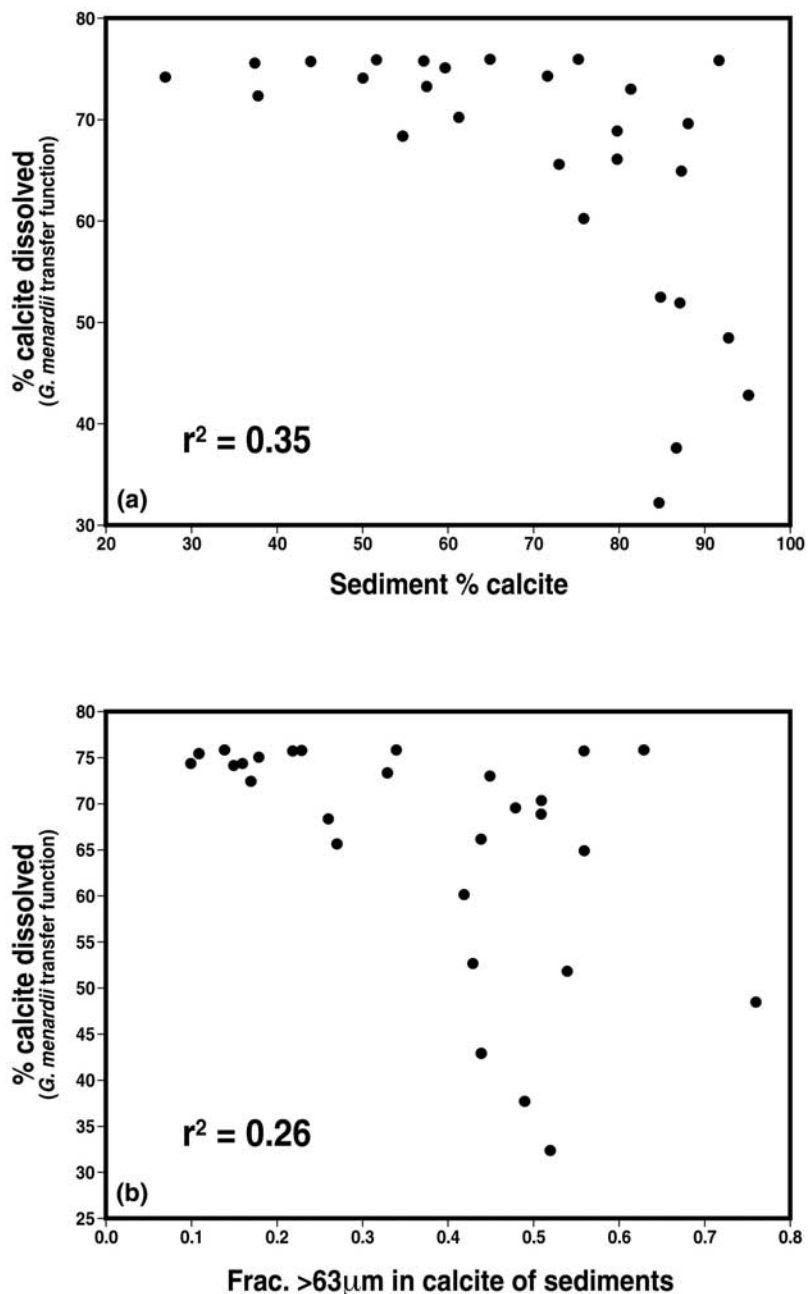


**Figure 9.** Percent calcite dissolved estimates from our *G. menardii* fragmentation index compared to sediment properties in the eastern equatorial Pacific. Data listings are given in Table 4. (a) Percent calcite dissolved plotted against sediment percent calcite. (b) Percent calcite dissolved plotted against coarse fraction (>63  $\mu\text{m}$ ) in the calcareous portion of the sediments. This demonstrates that the *G. menardii*-based estimates are not a function of these sedimentary properties.

counting shell fragments of *G. menardii* alone is sufficient for obtaining a linear relationship with carbonate dissolution and is not particularly labor intensive. To test for sediment composition bias in the *G. menardii* index, we measured sediment carbonate properties for a subset of our samples from the EEP (Table 4).

[45] For each of the 28 samples listed in Table 4, we weighed and analyzed a portion of bulk sediment for its calcium carbonate content using a Carlo Erba NA-1500

Analyzer (methods as in *Verardo et al.* [1990]). A second portion of each sample was weighed, disaggregated in distilled water and washed through a 63- $\mu\text{m}$  sieve. This greater than 63- $\mu\text{m}$  portion was weighed and analyzed for its calcium carbonate content also. This data allows us to compare the MFI to sediment carbonate content and to the grain size distribution of the carbonate.

[46] Figure 9 illustrates two plots: percent calcite dissolved calculated by our *G. menardii* index against total

percent calcite in the sediments (Figure 9a) and percent calcite dissolved calculated by our index against the coarse fraction ( $>63 \mu\text{m}$ ) in the calcareous portion of the sediments (Figure 9b). The scatter and lack of a linear trend in both of these plots show that our percent calcite dissolved estimates are not a function of these sediment properties. Hence, it does not appear that calcite content or grain size distribution exerts a strong influence on the *G. menardii* proxy.

## 7. Conclusions

[47] We developed a transfer function that can calculate percent calcite dissolved in samples using our *G. menardii* fragmentation index and biogeochemical model-derived values for percent calcite dissolved. Our transfer function produces a strong linear relationship for model-based and fragmentation-based percent calcite dissolved values between 35 and 75%. To examine the influence of biotic fluxes on the deep-sea carbonate record, we conducted three modeling experiments using sites from the eastern equatorial Pacific. These experiments demonstrate that calcite preservation reflects bottom water degree of saturation, organic carbon flux and the organic carbon to calcite flux ratio.

[48] Our index allows quantitative estimation of percent calcite dissolved and, with modeling, allows mapping of regional organic carbon to calcite flux ratios. This is valuable because direct measurements of the ratio are few [see *Klaas and Archer, 2002*]. However, our estimates of these ratio values depend on our estimates of percent calcite dissolved, which, in turn, depend on our calibration equation, which, ultimately, depends on accurate estimates of delta calcite, organic carbon flux and calcite flux for calibration locations. Nonetheless, the map gradients we found remain, even if the actual values of the ratio are uncertain. Thus, we are in a position to quantify both the direction and relative magnitude of changes in percent calcite dissolved through time. With quantitative information on organic carbon flux and with our *G. menardii* fragmentation data, we can in principle, reconstruct calcite fluxes and organic carbon to calcite flux ratios for the past, or for modern ocean areas where the data are lacking.

[49] **Acknowledgments.** We are very grateful to the curators and repositories that provided us with sediment samples and help in selecting cores for our work (June Padman, Oregon State University; Larry Peterson, RSMAS; Rusty Lotti-Bond, Lamont Doherty Earth Observatory; Warren Smith, Scripps Institution of Oceanography; and curators at the University of Hawaii). Thanks are also owed to the National Science Foundation for the support it provides to those repositories. We are also grateful to three anonymous reviewers for critiquing our manuscript thoroughly and constructively. We thank Mr. Mark Howland from Northern Illinois University for drafting our figures. This work was partially supported by NSF grant OCE -9617713 (Loubere), and the David and Lucille Packard Foundation and the Department of Energy Carbon Sequestration Program, Biological and Ecological Research (BER), U.S. Department of Energy DE-FG02-00ER63001 (Archer).

## References

Adelseck, C. G., Dissolution of deep-sea carbonate: Preliminary calibration of preservational and morphologic aspects, *Deep Sea Res.*, 25, 1167–1185, 1978.

Adelseck, C. G., and W. H. Berger, On the dissolution of planktonic for-

aminifera and associated microfossils during settling and on the seafloor, in *Dissolution of Deep Sea Carbonates*, vol. 13, edited by A. W. H. Be and W. H. Berger, pp. 70–81, Cushman Found. for Foraminiferal Res., Washington, D. C., 1975.

Anderson, D., and D. Archer, Glacial interglacial stability of ocean pH inferred from foraminifer dissolution rates, *Nature*, 416, 70–73, 2002.

Anderson, L. A., On the hydrogen and oxygen content of marine phytoplankton, *Deep Sea Res., Part 1*, 42, 1675–1680, 1995.

Archer, D. E., Modeling the calcite lysocline, *J. Geophys. Res.*, 96, 17,037–17,050, 1991a.

Archer, D. E., Equatorial Pacific calcite preservation cycles: Production or dissolution?, *Paleoceanography*, 6, 561–572, 1991b.

Archer, D. E., A data-driven model of the global calcite lysocline, *Global Biogeochem. Cycles*, 10, 511–526, 1996a.

Archer, D. E., An atlas of the distribution of calcium carbonate in sediments of the deep sea, *Global Biogeochem. Cycles*, 10, 159–174, 1996b.

Archer, D. E., and E. Maier-Reimer, Effect of deep sea sedimentary calcite preservation on atmospheric  $\text{CO}_2$  concentration, *Nature*, 367, 260–264, 1994.

Archer, D., S. Emerson, and C. Reimers, Dissolution of calcite in deep-sea sediments: pH and  $\text{O}_2$  microelectrode results, *Geochim. Cosmochim. Acta*, 53, 2831–2846, 1989.

Archer, D., A. Winguth, D. Lea, and N. Mahowald, What caused the glacial/interglacial atmospheric  $\text{PCO}_2$  cycles?, *Rev. Geophys.*, 38, 159–189, 2000.

Archer, D. E., J. L. Morford, and S. Emerson, A model of suboxic sedimentary diagenesis suitable for automatic tuning and gridded global domains, *Global Biogeochem. Cycles*, 16(1), 10.1029/2000GB001288, 2002.

Arrhenius, G., Sediment cores from the east Pacific, *Rep. Swed. Deep Sea Exped. 1947–1948*, 5, 1–228, 1952.

Bé, A. W. H., J. W. Morse, and S. M. Harrison, Progressive dissolution and ultrastructural breakdown in planktonic foraminifera, in *Dissolution of Deep Sea Carbonates*, vol. 13, edited by A. W. H. Be and W. H. Berger, pp. 27–55, Cushman Found. for Foraminiferal Res., Washington, D. C., 1975.

Behrenfeld, M., and P. Falkowski, Photosynthetic rates derived from satellite based chlorophyll concentration, *Limnology Oceanogr.*, 42, 1–20, 1997.

Berelson, W. M., et al., Biogenic matter diagenesis on the sea floor: A comparison between two continental margin transects, *J. Mar. Res.*, 54, 731–762, 1996.

Berger, W. H., Foraminiferal ooze: Solution at depths, *Science*, 156, 383–385, 1967.

Berger, W., Planktonic foraminifera: Selective solution and paleo-climatic interpretation, *Deep Sea Res.*, 15, 31–43, 1968.

Berger, W., Planktonic foraminifera: Selective solution and the lysocline, *Mar. Geol.*, 8, 111–138, 1970.

Berger, W., Deep-sea carbonates: Pleistocene dissolution cycles, *J. Foraminiferal Res.*, 3/4, 187–195, 1973.

Berger, W., Deep-sea carbonates: Dissolution profiles from foraminiferal preservation, in *Dissolution of Deep Sea Carbonates*, vol. 13, edited by A. W. H. Be and W. H. Berger, pp. 82–86, Cushman Found. of Foraminiferal Res., Washington, D. C., 1975.

Berger, W., Global maps of ocean productivity, in *Productivity of the Ocean: Present and Past*, edited by W. H. Berger, V. S. Smetacek, and G. Wefer, pp. 429–455, John Wiley, New York, 1989.

Berger, W., Pacific carbonate cycles revisited: Arguments for and against productivity control, in *Centenary of Japanese Micropaleontology*, edited by K. Ishizaki and T. Saito, pp. 15–25, Terra Sci., Tokyo, 1992.

Berger, W., and R. S. Keir, Glacial-Holocene changes in atmospheric  $\text{CO}_2$  and the deep-sea record, in *Climate Processes and Climate Sensitivity*, *Geophys. Monogr. Ser.*, vol. 29, edited by J. E. Hansen and T. Takahashi, pp. 337–351, AGU, Washington, D. C., 1984.

Berger, W., and J. Killingley, Box cores from the equatorial Pacific: C sedimentation rates and benthic mixing, *Mar. Geol.*, 45, 93–125, 1982.

Berger, W., K. Fischer, C. Lai and G. Wu, Oceanic productivity and organic carbon flux, I, in Overview and maps of primary production and export production, *Rep. 87-30*, pp. 1–45, Scripps Inst. of Oceanogr., Univ. of Calif., La Jolla, 1987.

Bramlette, M. N., Pelagic sediments in oceanography, in *Publ. Am. Assoc. Adv. Sci.*, 67, 345–366, 1961.

Broecker, W., Calcite accumulation rates and glacial to interglacial changes in ocean mixing, in *The Late Cenozoic Glacial Ages*, edited by K. K. Turekian, pp. 239–265, Yale Univ. Press, New Haven, Conn., 1971.

Broecker, W., Ocean chemistry during glacial time, *Geochim. Cosmochim. Acta*, 46, 1689–1705, 1982.

Broecker, W. S., and E. Clark, Carbonate size fractions: A paleocarbonate ion proxy, *Paleoceanography*, 14, 596–604, 1999.

- Broecker, W. S., and E. Clark, Reevaluation of  $\text{CaCO}_3$  size index paleo-carbonate ion proxy, *Paleoceanography*, 16, 669–671, 2001a.
- Broecker, W. S., and E. Clark, An evaluation of Lohmann's foraminifera weight dissolution index, *Paleoceanography*, 16, 531–534, 2001b.
- Chavez, F., and R. Barber, An estimate of new production in the equatorial Pacific, *Deep Sea Res.*, 34, 1229–1243, 1987.
- Codispoti, L., and J. Christensen, Nitrification, denitrification and nitrous oxide cycling in the eastern tropical South Pacific Ocean, *Mar. Chem.*, 16, 277–300, 1985.
- Emerson, S., and M. Bender, Carbon fluxes at the sediment-water interface of the deep sea: Calcium carbonate preservation, *J. Mar. Res.*, 39, 139–162, 1981.
- Hales, B., and S. Emerson, Calcite dissolution in sediments of the Ontong-Java Plateau: In situ measurements of pore water  $\text{O}_2$  and pH, *Global Biogeochem. Cycles*, 10, 527–541, 1996.
- Hales, B., and S. Emerson, Calcite dissolution in sediments of the Ceara Rise: In situ measurements of pore water  $\text{O}_2$ , pH, and  $\text{CO}_2$ , *Geochim. Cosmochim. Acta*, 61, 501–514, 1997a.
- Hales, B., and S. Emerson, Evidence in support of first-order dissolution kinetics of calcite in seawater, *Earth Planet. Sci. Lett.*, 148, 317–327, 1997b.
- Hedges, J. I., J. A. Baldock, Y. Gelin, C. Lee, M. L. Peterson, and S. G. Wakeham, The biochemical and elemental compositions of marine plankton: A NMR study, *Mar. Chem.*, in press, 2002.
- Jahnke, R. A., The global ocean flux of particulate organic carbon: Areal distribution and magnitude, *Global Biogeochem. Cycles*, 10, 71–88, 1996.
- Jahnke, R. A., D. B. Craven, and J.-F. Gaillard, The influence of organic matter diagenesis on  $\text{CaCO}_3$  dissolution at the deep-sea floor, *Geochim. Cosmochim. Acta*, 58, 2799–2809, 1994.
- Keir, R., The dissolution kinetics of biogenic calcium carbonate in seawater, *Geochim. Cosmochim. Acta*, 44, 241–252, 1980.
- Klaas, C., and D. E. Archer, Association of sinking organic matter with various types of mineral ballast in the deep sea: Implications for the rain ratio, *Global Biogeochem. Cycles*, 16, 10.1029/2001GB001765, in press, 2002.
- Ku, T.-L., and T. Oba, A method of quantitative evaluation of carbonate dissolution in deep-sea sediments and its application to paleoceanographic reconstruction, *Quaternary Res.*, 10, 112–129, 1978.
- Landry, M., J. Kirshtein, and J. Constantinou, Abundances and distributions of picoplankton populations in the central equatorial Pacific from  $12^\circ\text{N}$  to  $12^\circ\text{S}$ ,  $140^\circ\text{W}$ , *Deep Sea Res., Part II*, 43, 871–890, 1996.
- Le, J., and N. J. Shackleton, Carbonate dissolution fluctuations in the western equatorial Pacific during the Late Quaternary, *Paleoceanography*, 7, 21–42, 1992.
- Le, J., and R. C. Thunell, Modeling planktic foraminiferal assemblage changes and application to sea surface temperature estimation in the western equatorial Pacific Ocean, *Mar. Micropaleontol.*, 28, 211–229, 1996.
- Lohmann, G. P., A model for variation in the chemistry of planktonic foraminifera due to secondary calcification and selective dissolution, *Paleoceanography*, 10, 445–457, 1995.
- Loubere, P. W., Quantitative estimation of surface ocean productivity and bottom water oxygen concentration using benthic foraminifera, *Paleoceanography*, 9, 723–737, 1994.
- McMurtry, G., H. Veeh, and C. Moser, Sediment accumulation rate patterns on the northwest Nazca Plate, in *Nazca Plate: Crustal Formation and Andean Convergence*, edited by L. Kulm et al., *Mem. Geol. Soc. Am.*, 154, 211–249, 1981.
- Metzler, C. V., C. R. Wenkam, and W. H. Berger, Dissolution of foraminifera in the eastern equatorial Pacific: An in situ experiment, *J. Foraminiferal Res.*, 12, 362–368, 1982.
- Miao, Q., C. Thunell, and D. Anderson, Glacial-Holocene carbonate dissolution and the sea surface temperatures in the South China and Sulu Seas, *Paleoceanography*, 9, 269–290, 1994.
- Milliman, J. D., Production and accumulation of calcium carbonate in the ocean: Budget of a nonsteady state, *Global Biogeochem. Cycles*, 7, 927–957, 1993.
- Murray, J., and A. F. Renard, Report on deep-sea deposits based on specimens collected during the voyage of H.M.S. Challenger in the years 1873–1876, in *Report on the Scientific Results of the Voyage of HMS Challenger 1873–76*, Her Majesty's Stn. Off., Norwich, UK, 1891.
- Murray, J., R. Barber, M. Roman, M. Bacon, and R. Feely, Physical and biological controls on the carbon cycling in the equatorial Pacific, *Science*, 266, 58–65, 1994.
- Oba, T., Biostratigraphy and isotopic paleo-temperature of some deep-sea cores from the Indian Ocean, *Second Ser.Sci. Rep.* 41, pp. 129–195, Tohoku Univ., Sendai, Japan, 1969.
- Peterson, L. C., and W. L. Prell, Carbonate dissolution in recent sediments of the eastern equatorial Indian Ocean: Preservation patterns and carbonate loss above the lysocline, *Mar. Geol.*, 64, 259–290, 1985a.
- Peterson, L. C., and W. L. Prell, Carbonate preservation and rates of climatic change: An 800 kyr record from the Indian Ocean, in *The Carbon Cycle and Atmospheric  $\text{CO}_2$ : Natural Variations Archean to Present*, *Geophys. Monogr. Ser.*, vol. 32, edited by E. T. Sundquist and W. S. Broecker, pp. 251–269, AGU, Washington, D. C., 1985b.
- Peterson, M. N. A., Calcite: Rates of dissolution in a vertical profile in the central Pacific, *Science*, 154, 1542–1544, 1966.
- Redfield, A. C., On the proportions of derivatives in sea water and their relation to the composition of plankton, in *James Johnson Memorial Volume*, pp. 176–192, Univ. of Liverpool, Liverpool, England, 1934.
- Redfield, A. C., B. H. Ketchum, and F. A. Richards, The influence of organisms on the composition of seawater, in *The Sea*, vol. 2, edited by M. N. Hill, pp. 26–77, Wiley-Interscience, New York, 1963.
- Richards, F. A., Anoxic basins and fjords, in *Chemical Oceanography*, vol. 1, edited by J. P. Riley and D. Skirrow, pp. 611–645, Academic, San Diego, Calif., 1965.
- Ruddiman, W. F., Pleistocene sedimentation in the equatorial Atlantic: Stratigraphy and faunal paleoclimatology, *Geol. Soc. Am. Bull.*, 82, 283–302, 1971.
- Ruddiman, W. F., and B. C. Heezen, Differential solution of planktic foraminifera, *Deep Sea Res.*, 14, 801–808, 1967.
- Suess, E., and J. Thiede (Eds.), *Coastal Upwelling: Its Sedimentary Record*, Plenum, New York, 1981.
- Tans, P., I. Fung, and T. Takahashi, Observational constraints on the global atmospheric  $\text{CO}_2$  budget, *Science*, 247, 1431–1438, 1990.
- Thompson, P. R., and T. Saito, Pacific Pleistocene sediments: Planktonic foraminifera dissolution cycles and geochronology, *Geology*, 2, 333–335, 1974.
- Thunell, R. C., Optimum indices of calcium carbonate dissolution in deep-sea sediments, *Geology*, 4, 525–528, 1976.
- Thunell, R. C., and S. Honjo, Calcite dissolution and the modification of planktic foraminiferal assemblages, *Mar. Micropaleontol.*, 6, 169–182, 1981.
- Toggweiler, J., D. Dixon, and W. Broecker, The Peru upwelling and the ventilation of the south Pacific thermocline, *J. Geophys. Res.*, 96, 20,467–20,497, 1991.
- Verardo, D., P. Froelich, and A. McIntyre, Determination of organic carbon and nitrogen in marine sediments using the Carlo Erba NA-1500 Analyzer, *Deep Sea Res.*, 37, 157–165, 1990.

D. E. Archer, Department of Geophysical Sciences, University of Chicago, 5734 S Ellis Ave., Chicago, IL 60637, USA. (d-archer@uchicago.edu)

P. W. Loubere, Department of Geology and Environmental Geosciences, Northern Illinois University, De Kalb, IL 60115, USA. (paul@geol.niu.edu)

F. A. Mekik, Department of Geology, Grand Valley State University, Allendale, MI 49401, USA. (mekikf@gvsu.edu)